

## Crystalline $\text{Si}_3\text{N}_4$ thin films on Si(111) and the $4 \times 4$ reconstruction on $\text{Si}_3\text{N}_4(0001)$

Xue-sen Wang, Guangjie Zhai, Jianshu Yang, and Nelson Cue

*Department of Physics, The Hong Kong University of Science and Technology, Clear Water Bay, Kowloon, Hong Kong, China*

(Received 5 March 1999)

Crystalline silicon nitride ( $\text{Si}_3\text{N}_4$ ) thin films have been grown on Si(111) surfaces by exposing the substrate to  $\text{NH}_3$  at a temperature of  $\geq 1075$  K. An “ $8 \times 8$ ” electron diffraction pattern was observable even for a relatively thick  $\text{Si}_3\text{N}_4$  film. Images of the same surfaces obtained with a scanning tunneling microscope show surface superstructure with a period of 30.7 Å, and a minimum step height of 2.9 Å. These suggest the formation of  $\beta\text{-Si}_3\text{N}_4$ , with  $\text{Si}_3\text{N}_4(0001)\parallel\text{Si}(111)$ . The 30.7-Å periodic superstructure is attributed to the  $4 \times 4$  surface reconstruction on  $\text{Si}_3\text{N}_4(0001)$ . [S0163-1829(99)50428-1]

In recent years, silicon nitride has drawn wide attention in studies related to microelectronic applications.<sup>1,2</sup> Compared to  $\text{SiO}_2$ , silicon nitride and silicon oxynitride are expected to be more stable in a strong electric field and at a high working temperature. They should also be more effective as diffusion barriers to impurities such as boron. These make silicon nitride a promising candidate to replace  $\text{SiO}_2$  in metal-oxide-semiconductor field-effect transistor (MOSFET) and storage capacitors as the device scales continue to decrease in integrated circuits. In addition, high quality GaN has been grown recently on a silicon nitride film on Si(111).<sup>3</sup> This should lead to the prospect of integrating optoelectronic devices with silicon-based circuits. The growth mechanism of silicon nitride films on silicon and the morphology of the films, including the surface atomic structures, are important to these applications. Our current knowledge of these fundamental issues, however, is rather primitive.

Silicon nitride films can be grown on silicon by exposing a Si substrate to nitridation gases such as  $\text{NH}_3$  and  $\text{NO}$ ,<sup>4,5</sup> or to N atoms and ions.<sup>2,6-8</sup> Although  $\text{NH}_3$  molecules dissociate and react readily with Si surfaces at 300 K or even colder,<sup>4,9</sup> stoichiometric  $\text{Si}_3\text{N}_4$  films cannot form until the sample temperature is raised above 850 K for hydrogen desorption and Si out diffusion to occur.<sup>10,11</sup> The physical properties of silicon nitride films grown on Si have been analyzed with x-ray and ultraviolet photoelectron spectroscopy, Auger electron spectroscopy (AES), and low-energy electron diffraction (LEED).<sup>4-12</sup> After nitridation, the Si  $2p$  binding energy showed an increase of more than 2 eV. The Si LVV Auger peak shifted correspondingly from 91 to 84 eV. An “ $8 \times 8$ ” LEED pattern [the quotation marks are used to denote the periodicity on a silicon nitride surface with the basis of Si(111)] was observed on silicon nitride film grown on Si(111), indicating that a superstructure with periodicity of 30.7 Å ( $3.84 \text{ Å} \times 8$ ) exists on the film surface. But whether the film is crystalline  $\text{Si}_3\text{N}_4$  and what is the orientational relationship between the nitride film and Si substrate were unclear.

Recently, there have been scanning tunneling microscopy (STM) studies of silicon nitride film formation on Si(111).<sup>13-15</sup> In all of these STM studies, a 10.2-Å periodic structure was observed, which can be called a “ $8/3 \times 8/3$ ” reconstruction. The existence of this  $8/3$ -periodic structure can explain the fact that the  $(3/8, 0)$  spots of the “ $8 \times 8$ ”

LEED pattern were significantly brighter than other fractional spots. Nevertheless, the “ $8/3 \times 8/3$ ” reconstruction cannot lead to the whole “ $8 \times 8$ ” LEED pattern. Furthermore, the  $8/3$ -periodicity can hardly be correlated with the  $\text{Si}_3\text{N}_4$  crystal structure. Since the nitrated regions did not cover the whole surface in these STM studies, it was difficult to determine whether stoichiometric  $\text{Si}_3\text{N}_4$  films have been formed, or the observed features were the structure induced by the reaction of nitrogen with just the top layer of Si(111).

Here, we report on the results of our systematic experimental investigation in clarifying the above issues regarding silicon nitride thin film growth on Si(111). Our particular interests are in the possibility of crystalline silicon nitride film growth on silicon and the surface atomic structures on such films. The possibility of crystalline dielectric film growth on silicon could lead to the realization of multilayer integrated circuits and fabrication of devices made of other crystalline materials on Si substrates.<sup>16</sup> The surface structure of a dielectric thin film could have a strong influence on the growth of other materials above the film. We employed a combination of STM, LEED, and AES instruments to examine the features that appeared on the samples after exposure to  $\text{NH}_3$  and vacuum annealing. If crystalline silicon nitride films were formed, periodic surface atomic structures and flat terraces with atomic steps of specific heights would be observed. These features would be observable in later stages of film growth, not just at the beginning of nitridation. Furthermore, these particular features could be correlated with the known structure of silicon nitride crystals, and certain orientational relationship between the epitaxial film and the Si(111) substrate could be identified.

The experiments were conducted in an ultrahigh vacuum (UHV) system consisting of an analysis chamber and a sample preparation chamber separated by a gate valve. The analysis chamber (base pressure  $< 10^{-10}$  mbar) is equipped with a scanning tunneling microscope, a four-grid optics for LEED and AES. Both chambers are installed with electron bombardment heaters for sample annealing. The temperature of a Si sample during annealing was monitored with an accuracy of  $\pm 20$  K using an infrared pyrometer, with an appropriate emissivity correction. In the analysis chamber, Si(111) samples cut from nominally flat commercial wafers ( $n$ -type,  $\rho \sim 10 \Omega \text{ cm}$ ) and mounted on predegassed holders made of refractive metals were annealed at 1530 K for 1 min

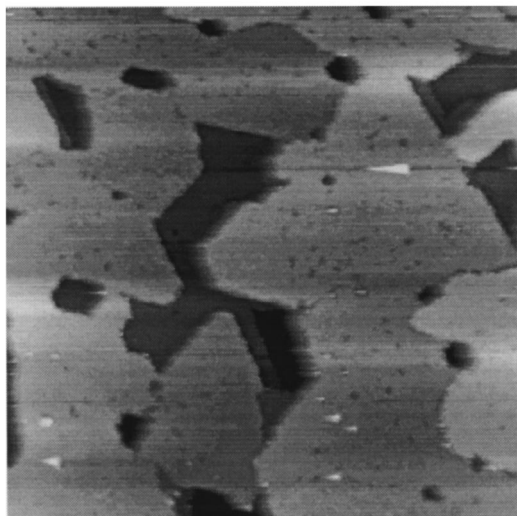


FIG. 1. 500 nm $\times$ 500 nm gray-scale STM image of silicon nitride film grown on Si(111) at 1175 K. The sample bias was +6.3 V and the tunneling current was 0.2 nA.

with chamber pressure below  $3 \times 10^{-9}$  mbar to get rid of oxide and other contaminants. After this procedure, the samples showed good surface order and no contamination as verified by LEED, STM, and AES. Nitridation was performed in the preparation chamber by introducing  $\text{NH}_3$  to the sample surface through a precision leak valve and a dosing tube. The sample was about 1 cm away from the tube exit during  $\text{NH}_3$  exposure. The pressure reading of the ion gauge in the preparation chamber was used as a qualitative monitor of the  $\text{NH}_3$  flux. The typical pressure reading was about  $3 \times 10^{-8}$  mbar during nitridation. The real pressure in front of the sample could be an order of magnitude higher than the ion gauge reading. The ratio of Auger peak height at 84 eV for nitrified Si to that at 91 eV for elemental Si was used as a rough quantitative measure of the nitride film thickness.<sup>17</sup> In such a self-nitridation of Si crystal, the nitride film thickness is limited to about 30 Å by the difficulty of Si diffusion through the film.<sup>10,11</sup> STM images were taken when the sample was cooled down to room temperature. The scales of LEED pattern and STM images were calibrated with the  $7 \times 7$  reconstruction and atomic steps on a Si(111) clean surface.

Figure 1 shows a STM image obtained on a Si(111) sample exposed to  $3 \times 10^{-8}$  mbar  $\text{NH}_3$  for 20 min at 1175 K. Terraces and steps characterizing a crystalline film are clearly seen. The ratio of the Auger peak height of nitrified Si to that of elemental Si is approximately 0.5 after such a nitridation. This Auger peak ratio changed little after further nitridation at the same condition, indicating a state of saturation. The estimated thickness of the nitride film is approximately 30 Å.<sup>10</sup> An “ $8 \times 8$ ” LEED pattern, as displayed in Fig. 2, has been observed for the nitride film. This LEED pattern indicates the existence of a surface periodic order, which also suggests that the film is crystalline. On the original flat Si(111) surface, there are roughly parallel monolayer atomic steps (3.14 Å in height) spaced about 250 nm on average. The locations and topology of the steps on the nitride films have no correlation with the steps on the original Si(111) surface. The minimum step height measured on the

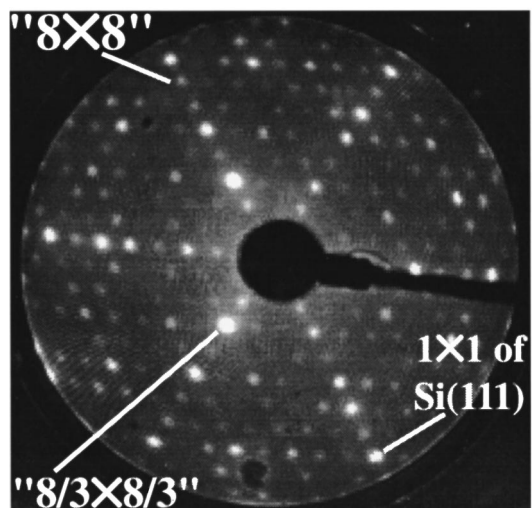


FIG. 2. LEED patterns observed for a silicon nitride film grown on Si(111) at 1175 K. The primary electron energy is 35 eV. The representative spots for Si(111)-( $1 \times 1$ ), “ $8 \times 8$ ,” and “ $8/3 \times 8/3$ ” periodicity are marked accordingly.

nitride film shown in Fig. 1 is  $2.9 \pm 0.1$  Å, which is equal to the lattice constant of  $\beta$ - $\text{Si}_3\text{N}_4$  in the  $[0001]$  direction. Many steps are twice or three times as high as the minimum-height step. On a clean Si(111) surface, steps of twice the monolayer height are rarely seen, and triple-layer steps can be found only when the average step spacing is  $\leq 150$  Å.<sup>18</sup> All of these indicate that a crystalline film different from the Si(111) substrate is formed after the high temperature nitridation. The step height data suggest that the film is  $\beta$ - $\text{Si}_3\text{N}_4$ , with  $\text{Si}_3\text{N}_4(0001) \parallel \text{Si}(111)$ .

Crystalline  $\text{Si}_3\text{N}_4$  can exist in two phases involving different stacking of the (0001) basal planes.<sup>19,20</sup> The trigonal  $\alpha$  phase has an  $ABCDABCD$  stacking with a  $c$ -axis period of 5.6 Å, while the hexagonal  $\beta$  phase has a relative simple  $ABAB$  stacking with a  $c$ -axis period of 2.9 Å. It is generally considered that the  $\alpha$  phase is a low-temperature phase and the  $\beta$  phase is stable at high temperature. Because sizable  $\text{Si}_3\text{N}_4$  single crystal is not available, there is no accurate determination of its physical properties, including its surface structure. The atomic configuration of the bulk-terminated  $\text{Si}_3\text{N}_4(0001)$  surface is sketched in Fig. 3. The diamond-shaped  $1 \times 1$  unit cell is drawn with dashed lines at the upper-right corner. The length of a side of the diamond is  $7.60 \pm 0.01$  Å,<sup>19</sup> which is about 1% less than twice the  $1 \times 1$  period on Si(111). Each layer of the  $1 \times 1$  cell consists of four N atoms and three Si atoms. One N atom (open or filled square in Fig. 3) forms bonds with three Si atoms in the (0001) plane, henceforth called horizontal N atom. The other three N atoms (open or filled triangles in Fig. 3) form bonds with Si atoms in a plane perpendicular to the horizontal plane, henceforth called vertical N atoms. The  $\text{Si}_3\text{N}_4$  crystal possesses threefold rotational symmetry with respect to  $[0001]$  axes passing through the horizontal N atoms ( $A$  and  $B$  sites) or the center of the hexagon (site  $C$ ). The good matches in lattice constants and in symmetry make the epitaxy of crystalline  $\text{Si}_3\text{N}_4$  film on Si(111) possible.

The “ $8 \times 8$ ” LEED pattern in Fig. 2 implies the existence of a surface superstructure with a periodicity of  $3.84 \times 8 = 30.7$  Å on the surface of the silicon nitride film. The spots

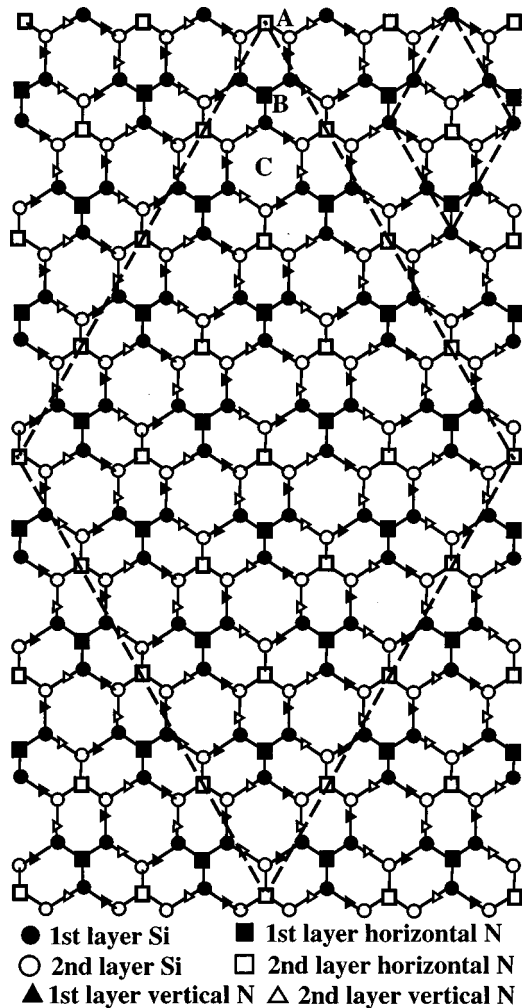
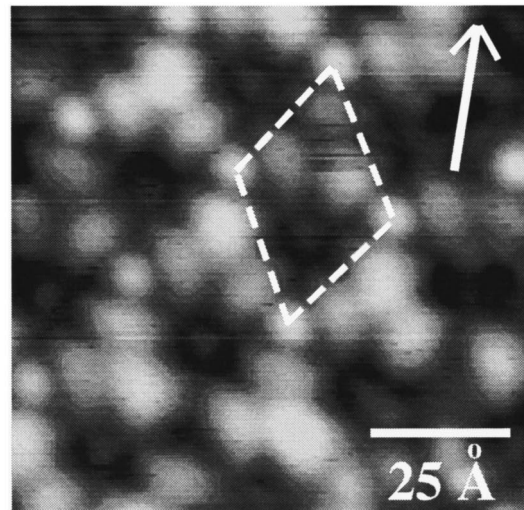


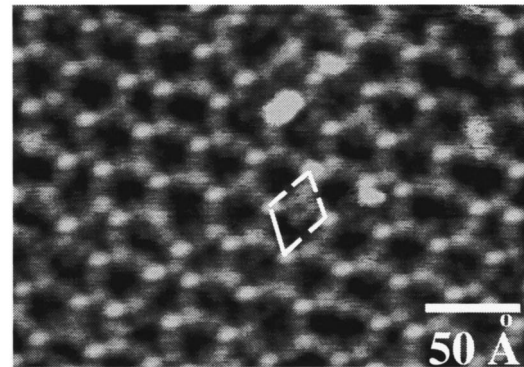
FIG. 3. Atomic configuration on bulk-terminated  $\beta$ - $\text{Si}_3\text{N}_4(0001)$  surface. The  $1 \times 1$  unit cell and the  $4 \times 4$  super cell are outlined with the small and large diamond, respectively. Three types of threefold symmetric sites are marked as A, B, and C.

marked as “ $8/3 \times 8/3$ ” are usually brighter than other fractional spots, which led previous investigators to believe that the surface periodicity is  $3.84 \text{ \AA} \times 8/3 = 10.2 \text{ \AA}$ .<sup>13</sup> Indeed, only the  $10.2\text{-\AA}$  periodic structure was observed in previous STM studies.<sup>13–15</sup> However, we have observed both the  $30.7\text{-\AA}$  and  $10.2\text{-\AA}$  periodic structures, depending on the sample preparation conditions. STM images of the  $30.7\text{-\AA}$  periodic structure on the  $\text{Si}_3\text{N}_4$  film are displayed in Fig. 4. We have observed this superstructure on samples prepared with  $\text{NH}_3$  exposure ranging from 1 min at  $1 \times 10^{-8}$  mbar [shown in Fig. 4(a)] to 20 min at  $3 \times 10^{-8}$  mbar [shown in Fig. 4(b)], with the substrate at  $T \geq 1075$  K. The ratio of Auger peak height of nitrated Si to that of elemental Si varied from 0.2 for a 1-min nitridation to 0.5 for a 20-min nitridation. These results indicate that the superstructure is intrinsic to the  $\text{Si}_3\text{N}_4(0001)$  surface, rather than just a chemisorption configuration on Si(111) in the early stage of nitridation. We assign this superstructure to the  $4 \times 4$  reconstruction on  $\text{Si}_3\text{N}_4(0001)$ , and emphasize that it is this  $\text{Si}_3\text{N}_4(0001)$   $4 \times 4$  reconstruction that generates the “ $8 \times 8$ ” LEED pattern.

Certain details of this  $\text{Si}_3\text{N}_4(0001)$   $4 \times 4$  reconstruction



(a)



(b)

FIG. 4. STM images of the  $4 \times 4$  reconstruction on  $\text{Si}_3\text{N}_4(0001)$  responsible for the “ $8 \times 8$ ” LEED pattern shown in Fig. 2. The  $4 \times 4$  unit cells are outlined with dashed-line diamonds. (a)  $95 \text{ \AA} \times 95 \text{ \AA}$  unoccupied-state image taken at  $V_s = +3.33$  V and  $I_T = 0.11$  nA, on a sample treated with a 1-min  $1 \times 10^{-8}$  mbar  $\text{NH}_3$  nitridation at 1075 K and a 2-min annealing at 1175 K. The arrow represents the  $[11\bar{2}]$  direction of Si(111) substrate. (b)  $275 \text{ \AA} \times 210 \text{ \AA}$  unoccupied-state image from a sample treated with a 20-min  $3 \times 10^{-8}$  mbar  $\text{NH}_3$  nitridation at 1175 K.

can be deduced from the unoccupied-state STM image in Fig. 4(a). The diamond-shaped unit cell as marked in the image has one bright circular dot at each apex. The unit cell can be divided into two equilateral triangles. In the upper triangle there are three higher-level protrusive complexes, and there is one lower-level slightly protruded feature in the middle of the lower triangle. In the occupied-state STM images (not shown), the upper triangle also appears brighter than the lower one. These indicate that the upper half of the unit cell is truly more elevated topographically than the lower half.

The area of the  $4 \times 4$  reconstruction unit cell is outlined as the large diamond on the bulk-terminated  $\text{Si}_3\text{N}_4(0001)$  surface model in Fig. 3. It involves several hundreds of atoms, which makes it extremely difficult to determine the atomic configuration of the reconstruction super cell. The exact atomic configuration at the  $\text{Si}_3\text{N}_4(0001)/\text{Si}(111)$  interface is also unknown. Nevertheless, our STM results have already

provided some clues for resolving these issues. For example, our STM images indicated that the orientation of the crystalline Si<sub>3</sub>N<sub>4</sub> film with respect to the Si substrate is unique: The [11 $\bar{2}$ ] direction of the Si substrate is along the longer diagonal of the 4×4 unit cell, pointing from the lower apex to the upper apex as marked in Fig. 4(a). STM images in Fig. 4 also show that the surface is threefold symmetric about a rotational axis passing an apex of the 4×4 cell. The possible locations of the apexes on the model surface in Fig. 3 are A, B, and C sites, because these sites all have threefold symmetry. If one type of the symmetric sites is chosen as the apex to draw the 4×4 diamond-shaped unit cell, it is easy to see that the upper and lower triangles are nonsymmetric about the short diagonal of the unit cell. When the A sites were the positions of the apexes, as sketched in Fig. 3, then a B site would be at the center of the upper triangle and a C site for the lower triangle. In other words, the apexes of the diamond and the centers of the upper and lower triangles are three different types of threefold symmetric sites. This is consistent with the STM image in Fig. 4(a) which shows that the centers of both the upper and lower triangles are threefold symmetric, but they are different from each other and from the apex sites. The consistency between the STM observation and the model structure provides additional support for our assignment of the 30.7-Å periodic structure to Si<sub>3</sub>N<sub>4</sub>(0001) 4×4 reconstruction.

Because of the complexity of the  $\beta$ -Si<sub>3</sub>N<sub>4</sub>(0001) 4×4 reconstruction, defects such as domain boundary and irregular unit cells have been quite abundant on the surfaces. Relatively good quality STM images of the 4×4 reconstruction were obtained after NH<sub>3</sub> exposure at 1175 K followed by UHV annealing at the same temperature for 2–5 min. Even then, the sizes of the 4×4 domains were on the order of 100 Å. We are still searching for the proper preparation conditions to improve the surface order.

In addition to the 4×4 reconstruction, we have also observed the 10.2-Å periodic structure, i.e., the “8/3×8/3” reconstruction, on Si(111) exposed to 1×10<sup>-8</sup> mbar NH<sub>3</sub> for 1 min at 1075 K. When annealed at 1175 K for a few minutes, the 10.2-Å periodic area was converted to the 4×4 reconstruction. We have noticed that, if the purity of NH<sub>3</sub> used for nitridation degrades, the “8/3×8/3” structure persists and the transition to the 4×4 cannot happen. The impurity in the degraded NH<sub>3</sub> gas has not been identified because its level is below our detection limit. It could be oxygen or water vapor. The degree of nitridation is severely hindered by the impurity. AES measurements showed that, after a 20-min 3×10<sup>-8</sup> mbar degraded-NH<sub>3</sub> exposure at 1175 K, the height ratios of the N peak and the nitrided Si peak to the elemental Si peak decreased by a factor of 3, and 2, respectively, compared to the case using purer NH<sub>3</sub>. The more severe decrease of the N peak indicates that the stoichiometry of the “8/3×8/3” and the 4×4 structures are different.

For comparison, we have also examined the surface morphology of Si(001) samples after the similar nitridation processing. The initial order on Si(001) was destroyed gradually by the nitridation, and no surface order was observed eventually. The nitride films grown on Si(001) were completely amorphous. The lack of proper matches in surface lattice constants and in symmetry makes crystalline silicon nitride growth impossible on Si(001).

In summary, we have observed crystalline silicon nitride film growth on Si(111) after NH<sub>3</sub> exposure at  $T \geq 1075$  K. STM measurements suggest that the film is  $\beta$ -Si<sub>3</sub>N<sub>4</sub>, with Si<sub>3</sub>N<sub>4</sub>(0001)||Si(111). A 4×4 reconstruction has been observed on the Si<sub>3</sub>N<sub>4</sub>(0001) surface, which yields the “8×8” LEED pattern.

This work was partially supported by the Research Grant Council of Hong Kong SAR (Grant No. HKUST6127/97P).

- <sup>1</sup>M. Arienzo and W. A. Orr-Arienzo, in *Preparation and Properties of Silicon Nitride Based Materials*, edited by D. A. Bonnell and T. Y. Tien, Materials Science Forum Vol. 47 (Trans Tech Publications, Zürich, 1989), p. 228.
- <sup>2</sup>T. P. Ma, IEEE Trans. Electron Devices **45**, 680 (1998).
- <sup>3</sup>Y. Nakada, I. Aksenov, and H. Okumura, Appl. Phys. Lett. **73**, 827 (1998).
- <sup>4</sup>Ph. Avouris, F. Bozso, and R. J. Hamers, J. Vac. Sci. Technol. B **5**, 1387 (1987); Ph. Avouris and R. Wolkow, Phys. Rev. B **39**, 5091 (1989).
- <sup>5</sup>M. D. Wiggins, R. J. Baird, and P. Wynblatt, J. Vac. Sci. Technol. **18**, 965 (1981).
- <sup>6</sup>D. V. Tsu, G. Lucovsky, and M. J. Mantini, Phys. Rev. B **33**, 7069 (1986).
- <sup>7</sup>D. Bolmont, J. L. Bischoff, F. Lutz, and L. Kubler, Appl. Phys. Lett. **59**, 2742 (1991).
- <sup>8</sup>J. F. Delord, A. G. Schrott, and S. C. Fain, Jr., J. Vac. Sci. Technol. **17**, 517 (1980).
- <sup>9</sup>F. Bozso and Ph. Avouris, Phys. Rev. B **38**, 3937 (1988).
- <sup>10</sup>C. Maillot, H. Roulet, and G. Dufour, J. Vac. Sci. Technol. B **2**, 316 (1984).
- <sup>11</sup>C. H. F. Peden, J. W. Rogers, Jr., N. D. Shinn, K. B. Kidd, and K. L. Tsang, Phys. Rev. B **47**, 15 622 (1993).
- <sup>12</sup>G. Rangelov, J. Stober, B. Eisenhut, and Th. Fauster, Phys. Rev. B **44**, 1954 (1991).
- <sup>13</sup>E. Bauer, Y. Wei, T. Müller, A. Pavlovskaya, and I. S. T. Tsong, Phys. Rev. B **51**, 17 891 (1995).
- <sup>14</sup>M. Yoshimura, E. Takahashi, and T. Yao, J. Vac. Sci. Technol. B **14**, 1048 (1996).
- <sup>15</sup>B. Röttger, R. Klieise, and H. Neddermeyer, J. Vac. Sci. Technol. B **14**, 1051 (1996).
- <sup>16</sup>R. A. McKee, F. J. Walker, and M. F. Chisholm, Phys. Rev. Lett. **81**, 3014 (1998).
- <sup>17</sup>G. Lucovsky (unpublished).
- <sup>18</sup>J. Wei, X.-S. Wang, J. L. Goldberg, N. C. Bartelt, and E. D. Williams, Phys. Rev. Lett. **68**, 3885 (1992).
- <sup>19</sup>D. R. Messier and W. J. Croft, in *Growth Mechanisms and Silicon Nitride*, edited by E. R. Wilcox (Marcel Dekker, New York, 1982), p. 131.
- <sup>20</sup>M. Mitomo, in *Silicon Nitride*, edited by S. Somiya, M. Mitomo, and M. Yoshimura (Elsevier, London, 1990), p. 1.